(Received 21 August 2024, Accepted 27 September 2024, Scheduled 25 October 2024)

Research on Wireless Signal Coverage Enhancement in Mine Tunnels with Different Turning Angle Based on PRIS

Bo Yin[1], Xiaoliang Li[1,*], Yun Li[2,3], and Xiangdong Fu[1]

[1] School of Optoelectronic Engineering, Chongqing University of Posts and Telecommunications, Chongqing, China
[2] Chongqing Research Institute, China Coal Technology & Engineering Group, Chongqing, China
[3] State Key Laboratory of Coal Mine Disaster Prevention and Control, Chongqing, China

ABSTRACT: Wireless communication is an essential part of future smart mines. However, the complex structure of mines, especially curved mine tunnels, makes the coverage of wireless signals drastically reduced compared to the ground, which increases the difficulty of wireless communication inside the mine. In order to improve the transmission characteristics of wireless signals in the underground non-line-of-sight (NLOS) region, a new passive reconfigurable intelligent metasurface (PRIS) is proposed, which realises the reconfigurable characteristics of the PRIS beam through the principles of passive coding and splicing, and can be applied to different turning angle tunnels. Finally, the PRIS with different radiation directions is designed and simulated in the simulation software, and loaded into different turning angle tunnels for the simulation of tunnel power distribution. By comparing with the simulation results of unloaded PRIS, the PRIS is the most effective when the turning angle is 50°. The overall power intensity of the tunnel is improved by 25 dBm, and the overall power intensity of the tunnel is improved by $14 \sim 17$ dBm at other turning angles, which proves the effectiveness of passive splicing metasurface in the application of underground wireless communication blindness mending scenarios.

1. INTRODUCTION

The advancement of wireless communication technology has greatly facilitated the exploitation of mining resources. However, the operational viability of these technologies is contingent upon the signal power strength in diverse scenarios, which must reach the minimum communication limit [1, 2]. However, the complex structure of underground passages in mines presents significant challenges to the propagation of electromagnetic energy carrying base station signals, which encounter substantial obstacles in the form of mine walls and are unable to propagate properly. In non-line-of-sight (NLOS) scenarios, there may be weak communication or even blind areas in any radio communication frequency [3, 4]. It is therefore imperative that steps be taken to improve the signal coverage of underground wireless communication systems. In order to achieve enhanced coverage, it is common practice to deploy large-scale small base stations for the secondary radiation of electromagnetic energy [5, 6]. The deployment of Leaky Feeder Communication System (LFCS) and fibre optic communications can also be applied to mine communications [7]. These methods rely on complex active devices, and an increase in the number of devices will lead to more complex control algorithms, complicating hardware and software systems and leading to high costs. Repeaters represent an effective method of improving signal coverage [8, 9]. One type of repeater is a metal reflector, comprising metal plates or balls. However, the high attitude and inflexible waveform control due to Snell's law limit its application. Another type is a dual antenna system, whereby the signal received by the receiving antenna can be controlled by the transmitting antenna over a wide range of angles [10–13].

It can be observed that the fundamental objective of the aforementioned two repeater methods is to facilitate the transformation of an NLOS scenario into a line-of-sight (LOS) scenario. The deployment of these two repeaters in NLOS scenarios necessitates the utilisation of a multitude of passive or active structures, distributed in a manner that ensures reasonable coverage within complex underground tunnels. A metasurface is a planar artificial structure comprising an ordered arrangement of subwavelength meta-atoms, which can modulate electromagnetic waves emitted from a base station antenna with high efficiency and accuracy. It offers a novel approach to wireless communication in mines, representing a significant departure from the use of repeaters [14–18]. This paper proposes a scheme to enhance mine NLOS signal coverage in the 5G-6G band, using the metasurface concept and hardware design.

Due to the limited diffraction capacity of high frequency electromagnetic waves, tunnels with different curvatures can block signals from base stations. If we configure a thin, low-cost, lightweight passive metasurface on the tunnel wall to deflect incoming signals, the blocked NLOS area can be used for effective communication. It is notable that passive metasurface presents a substantial cost advantage for this pervasive corner. The deflection of the incident wave at a specific angle towards the NLOS region represents a viable concept. Deflecting the incident wave to a specific angle pointing to the NLOS region is just a concrete idea. However, the turning angles of each tunnel underground are different, and a single passive metasur-

* Corresponding author: Xiaoliang Li (1433853747@qq.com).

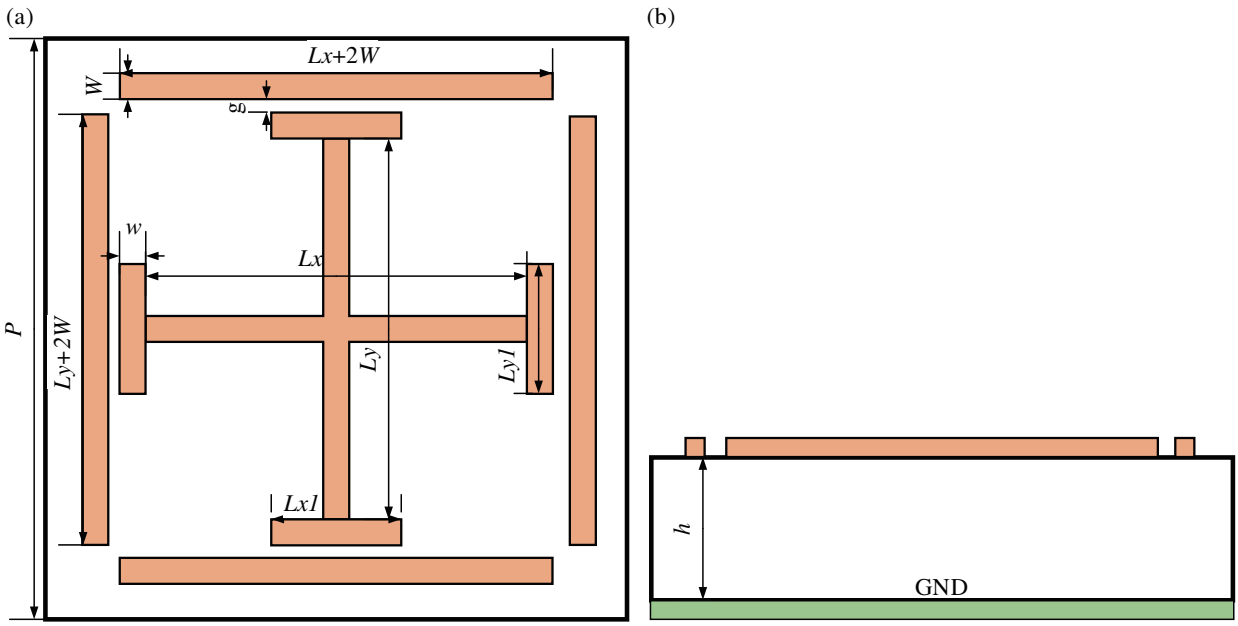

FIGURE 1. Schematic of metasurface unit structure: (a) Top view; (b) survey view.

face is not suitable for signal coverage enhancement in tunnels with different turning angles. Therefore, how to use the passive metasurface to improve the signal coverage characteristics in the blind area of wireless signal coverage in tunnels with different turning angles has always been the concern of researchers. In [19], Yi et al. put forward a method for achieving signal coverage which involved using a wide beam deflected into the NLOS region of an L-shaped corridor with a flat scattering pattern, which is less susceptible to blockages. In [20], Guo et al. put forth a proposal for a multiple reflective Reconfigurable Intelligent Metasurface (RIS) as a potential solution to the NLOS signal blinding issue caused by mine collapse or curved tunnels. In [21], Xue et al. advanced a concept for a reflective RIS that could potentially reduce the number of p-i-n diodes needed by up to 60% by optimising the elements and arrays of the metasurface through the use of an algorithm to enhance the signal coverage of wireless communication. The aforementioned studies on the utilisation of metasurfaces in wireless communication blind coverage predominantly concentrate on conventional indoor and corridor scenes. Conversely, there is a paucity of research exploring NLOS blind area in the context of complex and dynamic tunnel environments beneath mines. Furthermore, the explosion-proof specifications for subterranean applications are particularly rigorous, and the demands placed on active devices are considerable. Accordingly, in this paper, the use of metasurfaces in underground mine tunnels will be extended by array splicing, so that Passive Reconfigurable Intelligent Metasurface (PRIS) can be applied to the signal coverage of mine tunnels with different turning angles by simple splicing.

Here, we propose a splicable PRIS. Compared with the traditional reflective metasurface, it is more applicable in the mine tunnel. The paper is structured as outlined below. Section 2 presents the design of the "Jerusalem" unit. Section 3 expounds on the methodology and fundamental principles underlying the splicable PRIS. Section 4 presents the simulation outcomes of the splicable PRIS, alongside an assessment of the power intensity within the mine tunnel, thereby validating the efficacy of this innovative technology for underground mine tunnel applications. The analysis underscores the splicable PRIS as an attractive solution for addressing mine tunnel blinding challenges. Lastly, Section 5 summarizes the key findings and conclusions of the paper.

2. DESIGN OF METASURFACE UNITS

In order to make the metasurface unit more suitable for the mine situation, the classical "Jerusalem" square ring structure [22] is chosen in this paper, and by using the structure of the unit with multiple oscillators, a phase shift range of 330° and a phase shift curve with good linearity can be obtained by only changing the size of the patch. As shown in Fig. 1, the top and side views of the element of the reflection array are given. The reflection array element is printed on a grounded substrate F4B having a relative dielectric constant of 2.2 and a dielectric loss angle tangent of 0.007. The relationship among the lengths L, L_x, and L_y is determined by (1), and the values of the specific variables of this element are shown in Table 1.

$$L = 2 * L_x = 2 * L_y \tag{1}$$

TABLE 1. Structural parameters of the square ring of Jerusalem.

Parameters	Element Dimension and Descriptions	
	Dimensions (mm)	Descriptions
D	17	Media plate thickness
h	3	Unit period
w	0.5	Oscillator width
g	0.6	Gap width

By using periodic boundaries and the Flouquet model, the reflection phase and amplitude of the unit are varied by changing the arm length of the patch in the CST simulation software.

As can be seen in Fig. 2, the range of variation of the unit reflection phase is greater than 330°, and the reflection amplitude is greater than 0.95. The linearity of the curve with the length of the unit patch is good. Therefore, the proposed Jerusalem structure with accompanies oscillators has great potential for complex mine wireless signal coverage.

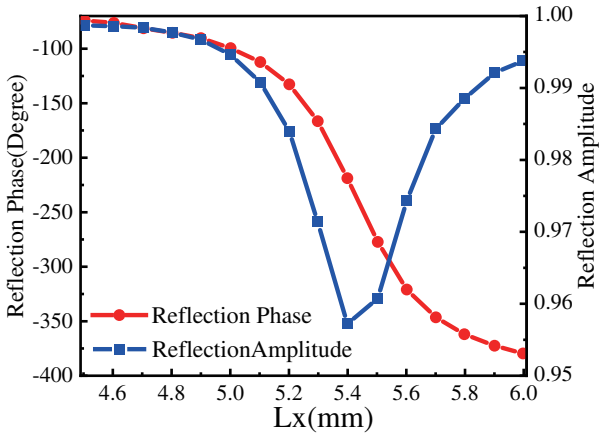

FIGURE 2. Phase and amplitude curves of reflections from the PRIS unit.

3. DESIGN OF RECONFIGURABLE PRIS SUITABLE FOR MINE NLOS SIGNAL COVERAGE

3.1. Passive Splicing Metasurface Design Theory Based on Bit Phase Quantisation

For a planar reflective metasurface with the beam pointing in the azimuthal plane as θ_a, the phase gradient p_g of each unit on the metasurface is:

$$p_g = k_0 \sin\theta_\alpha \tag{2}$$

a penumbral or shaped beam excited by a plane wave, it can be seen from Eq. (2) that the beam pointing θ_{a0} is determined by the phase gradient p_g. Assume that there are two kinds of subarrays with different phase gradients, which are represented by the numerical symbols 0 and 1 in the 1-bit phase quantisation principle, in which the phase gradient of 0 is p_{g0}, the beam pointing to θ_{a0}, and the phase gradient of 1 is p_{g1}, the beam pointing to θ_{a1}. According to the interpolation theory, the combination of several 0 and 1 can be used to get the array with equivalent phase gradient p_{gi}, in which the variation range of p_{gi} is $[p_{g0}, p_{g1}]$. As the equivalent phase gradient p_{gi} changes, the beam pointing θ_{ai} can be theoretically obtained as any value in the range $[\theta_{a0}, \theta_{ai}]$. In order to determine the subarray splicing method with beam pointing to θ_{ai}, the principle of average phase gradient is proposed in this paper. Assuming that the array consists of M subarrays 0 and N subarrays 1, the array can be denoted as a row vector V, which contains N elements 0 and M elements 1. The total phase shift of the array after splicing is ψ_{all}.

$$\psi_{all} = 2\pi(M+N) \tag{3}$$

The average phase gradient is defined as:

$$\bar{p_g} = \frac{\psi_{all}}{L(V)} \tag{4}$$

where $L(V)$ is the physical length of the array along the azimuthal direction. To make the beam point to θ_{ai}, the approximation error ε needs to be small enough according to Eq. (4), and then the array V can be considered to be constructed through M subarrays 0 and N subarrays 1 to make the beam point to the desired value θ_{ai}:

$$\varepsilon = |p_{gi} - \bar{p_g}| \tag{5}$$

Through passive subarray splicing, the array elements in a cycle are used as subarrays, by splicing multiple subarrays, the metasurface array can be extended to the desired aperture while keeping the phase gradient and beam pointing unchanged. Therefore, this PRIS technology has the reconfigurable and intelligent functions of RIS, it can real-time stitch the metasurface arrays according to the changes of the external environment and realise reconfigurable beam pointing, and it is a completely passive design, which can be realised on a large scale and has the advantages of low-cost, low-power consumption and low complexity.

3.2. Splicing PRIS Design

The passive RIS in this paper consists of 2 subarrays with different phase gradients, which are denoted by 1-bit numerical symbols "0" and "1", respectively, with "0" denoting a uniform phase-gradient subarray with beam pointing to θ_{a0} and "1" denoting the uniform phase gradient subarray with beam pointing to θ_{a1}. The phase variation of each unit of each subarray along the x-direction ranges over exactly one phase cycle, i.e., the phase variation from the first array element to the first array element of the next cycle is 2π, and the phase variation of each unit of the subarray along the y-direction is 0, i.e., each unit is kept the same along the pitching direction, as shown in Fig. 3. According to the principle of average phase gradient, the M_S subarrays 0 and N_S subarrays 1 are arranged in an orderly manner to form the minimum period row vector $V_{\min}$ in the reflecting array array, and M_S and N_S are integers greater than or equal to zero. In order to make this minimum period row vector $V_{\min}$ the main beam pointing to θ when the frequency is f, according to the specific application scenario, the minimum period row vector $V_{\min}$ is used as the unit to arrange the period in the x-direction of the array for the purpose of reconstructing the reflected beam from the metasurface. In order to make the reconstructed beam pointing range of PRIS satisfy [48°, 72°], the beam pointing of the arrays consisting of subarrays 0 and 1 should be chosen around 48° and 72°, respectively.

In order to verify that the passive RIS can achieve beam reconfiguration, the array beam pointing is designed to be 64°. From Eq. (5), the maximum error $\varepsilon = 0.5$ when one subarray 0 and four subarrays 1 form the minimum row vector $V_{\min}$, and this error is within the controllable range of the requirements for blinding the mine tunnel. Combined with the simulation software to calculate the simulation beam pointing of

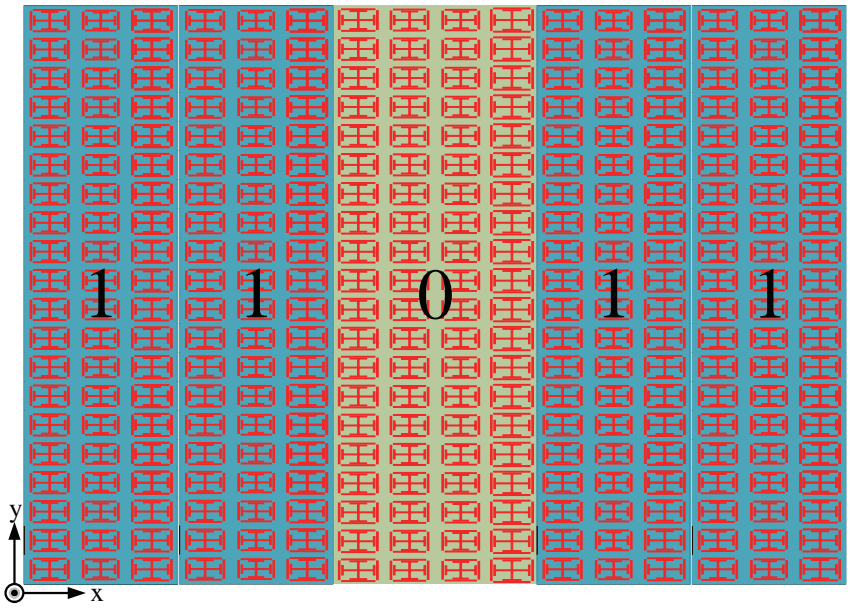

FIGURE 3. Principle of passive splicing RIS regulation.

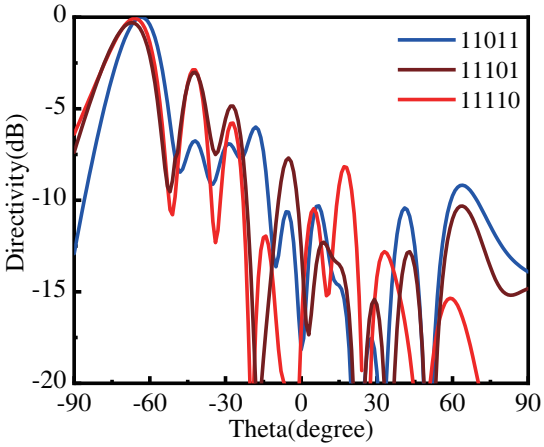

FIGURE 4. Simulated beam pointing at 64°.

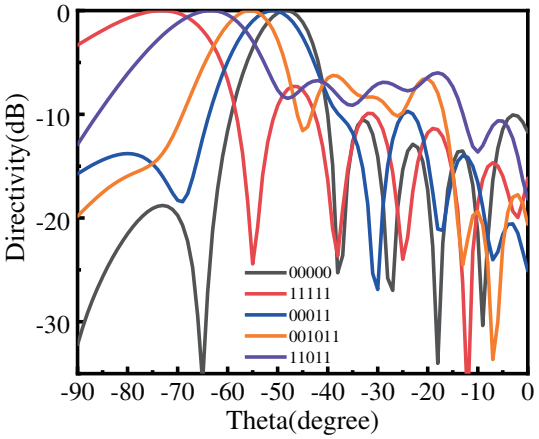

FIGURE 5. Simulated directional maps for 5 sets of different vector V beam pointing.

TABLE 2. Full-wave simulation results for 5 sets of different vector V beam pointing.

$V_{\min}$	θ Full-wave simulation value
00000	48°
00011	52°
001011	57
11011	64°
11111	72°

$V_{\min}$ as shown in Fig. 4, the three arrangements are compared, and considering the beam pointing and sub-flap level, the array with $V_{\min} = [11011]$ and an exit angle of 64° is selected for enhancing coverage in blind areas of wireless signals.

To further substantiate the veracity of the average phase gradient principle in estimating beam pointing accuracy, we undertake an in-depth verification process. The full-wave simulation results of the beam pointing of five different vectors V are given in Table 2 and Fig. 5, and the most suitable group is selected by combining with the subvalve level. The simulated values of the beam pointing for these five vectors V are 48°, 52°, 57°, 63°, and 72°, which basically satisfy the reconfigurable range of beam pointing of [48°, 72°].

4. SIMULATION OF SIGNAL COVERAGE IN BLIND ZONE OF CURVED TUNNEL WITH DIFFERENT TURNING ANGLES

In practical underground tunnel communication scenarios, the propagation space for electromagnetic waves is distinctly categorized into near-field and far-field regions. The delineation between these two zones is precisely determined by Eq. (6):

$$dp = \text{maximun}\left(\frac{a^2}{\lambda}, \frac{b^2}{\lambda}\right) \tag{6}$$

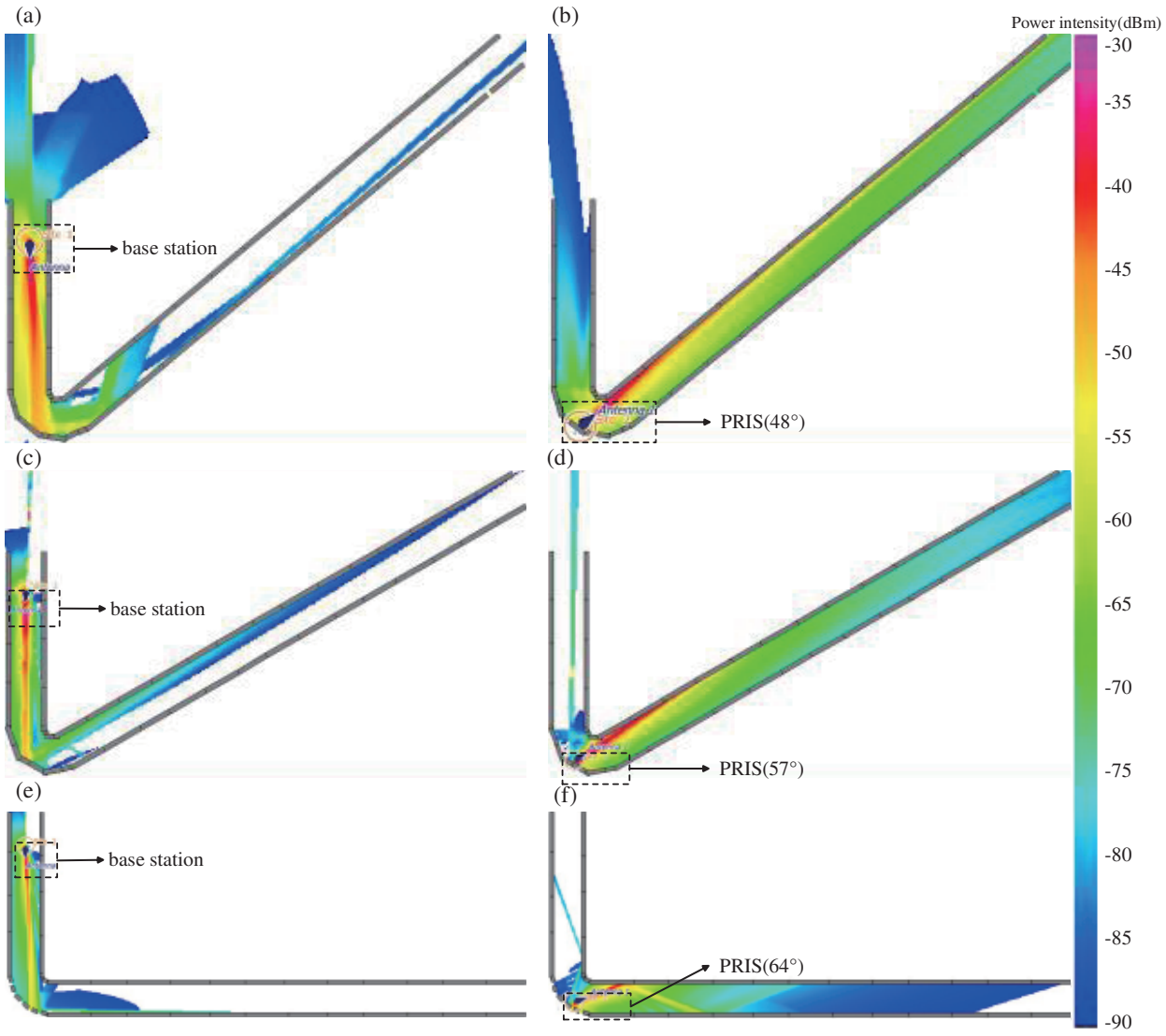

FIGURE 6. Simulation of the signal coverage of the mine tunnel with different turning angles. (a) 50° without PRIS. (b) 50° with PRIS. (c) 70° without PRIS. (d) 70° with PRIS. (e) 90° without PRIS. (f) 90° with PRIS. The power level below −90 dBm is marked as white.

a and b are the length and width of the mine tunnel, and from the formula, we calculate that the blinding area of the tunnel is the near-field region, in which the electromagnetic wave is mostly multi-mode propagation, similar to the propagation mode of free space. Therefore, we use the free-space wave propagation loss model for the near-field region and combine it with the ray-tracing method for analysis.

The ray tracing method in Altair WinProp is used to simulate the electromagnetic wave transmission in the tunnel with different turning angles. The passive reflective device can be equivalent to an active base station located at the corner position. In the actual underground tunnel environment, the incident wave from the base station to the passive reflector array is approximated as an obliquely incident plane wave, and the equivalent omnidirectional radiated power of the equivalent active base station is:

$$EIRP = \frac{T_{BS\_}EIRP}{4\pi d^2} RCS_A(\theta, \varphi) \tag{7}$$

where $RCS_A(\theta, \varphi)$ denotes the antenna RCS direction map; $T_{BS\_}EIRP$ denotes the signal source transmit power; and d denotes the distance from the signal source to the PRIS.

The signal coverage of the mine tunnel mainly consists of wall reflections as well as direct radiation from the transmitting source to the receiving source. Using the equivalent radiation source model, we set the EIRP of the reflective element surface, import the antenna radiation direction map of the passive RIS, and set the relevant electromagnetic parameters of the mine tunnel, as shown in Table 3.

The power distribution simulation analysis is carried out for the tunnel with turning angles of 50°, 70°, and 90°. Due to the complex electromagnetic environment in mine tunnels, with current technological means, the minimum received power intensity required by terminal devices must reach −90 dBm, and after simulation analysis, the comparison of power intensity before and after loading the PRIS in mine tunnels with varying angles is illustrated in Figs. 6(a)–(f).

TABLE 3. Tunnel structure and electromagnetic parameter setting.

Sectional Parameters of the Mine tunnel (m)			Radio Transmission Parameters (dB)		
Length	Width	Height	Reflective Loss	Transmission Loss	Number of Ray Traces
2	3.2	2.5	9	40	5

It can be seen that the signal strength in the NLOS region in the tunnel loaded with the passive RIS is significantly enhanced. To explain the function of the PRIS more clearly, the power intensity at different positions on the tunnel (expressed as the distances from the corner to different positions) can be quantitatively analyzed, and the results are shown in Fig. 7.

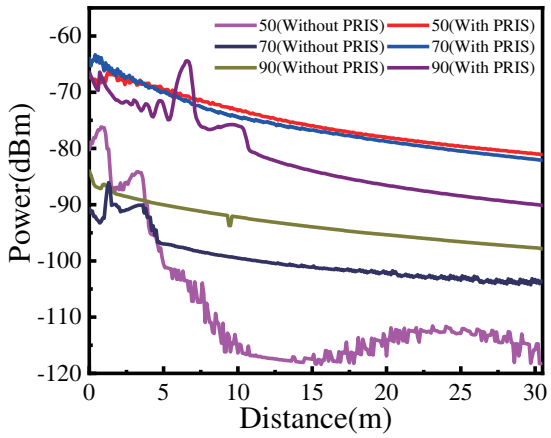

FIGURE 7. Signal strength analysis of electromagnetic wave propagation in a curved tunnel with different angles.

As can be seen from the power intensity comparison graph in Fig. 7, it can be seen that when the turn angle of the tunnel is 50°, the power intensity in the blind area after loading PRIS increases most obviously, about 25 dBm, and the intensity distribution is more uniform, which is because the turning angle of the tunnel is small. When the tunnel structure is complex, the reflection of electromagnetic wave is more complicate, and the Multipath Effect is more serious, which greatly reduces the transmission distance of the electromagnetic wave. PRIS effectively directs the electromagnetic wave signals from the base station, greatly reducing the Multipath Effect. Similarly, when the turning angle of the tunnel is 70° and 90°, the power intensity in the blind zone is increased by 15–20 dBm after loading PRIS.

5. CONCLUSION

A novel beam-pointing reconfigurable PRIS is proposed and applied to enhance the signal coverage in the blind zone of wireless communication in tunnels with different turning angles. By utilising passive coding and splicing principles, the PRIS was made beam reconfigurable in [48°, 72°]. Finally, three different splicing methods combined into the PRIS are selected to enhance the wireless signal coverage in the blind zone of the tunnels with different turning angles. The simulation results show that the power intensity in the blind zone after loading PRIS is most obvious when the turning angle of the tunnel turn is 50°. The power intensity is increased by about 25 dBm, and the power intensity in the blind zone after loading PRIS is increased by 15–20 dBm when the turning angle of the tunnel turn is 70° and 90°. By comparing and analysing the simulation results, the effectiveness of PRIS in enhancing the wireless signal coverage in underground mine is proved and lays a solid foundation for the application of PRIS in mine tunnel wireless communication.

ACKNOWLEDGEMENT

This work was supported by the Open Fund Project of State Key Laboratory of Gas Disaster Monitoring and Emergency Technology (2022SKLKF12).

REFERENCES

[1] Yang, S., "Development trend of intelligent underground mining of coal mine," *Inner Mongolia Coal Economy*, Vol. 3, 160–162, 2023.

[2] Shen, X., C. Liu, and N. Kong, "Research on the technical development status of the intelligent mine base on internet of things," *China Mining Magazine*, Vol. 27, No. 7, 120–125, 2018.

[3] Ma, L., "Study on intelligent mine based on the application of 5G wireless communication system," in *IOP Conference Series: Earth and Environmental Science*, Vol. 558, No. 3, 032050, 2020.

[4] Huang, L., "Application of intelligent safety monitoring system in mining engineering," *China Metal Bulletin*, Vol. 1, 29–31, 2023.

[5] Hu, H. Z., Z. G. Du, N. Chu, *et al.*, "Key technologies of personnel positioning system based on smart mining platform," *Coal Mine Safety*, Vol. 152, 134–138, 2021.

[6] Farjow, W., K. Raahemifar, and X. Fernando, "Novel wireless channels characterization model for underground mines," *Applied Mathematical Modelling*, Vol. 39, No. 19, 5997–6007, 2015.

[7] Issa, A., N. Hakem, and N. Kandil, "Combining leak feeder cable and antenna to support mobile network in underground mine environment," in *2020 IEEE International Symposium on Antennas and Propagation and North American Radio Science Meeting*, 1133–1134, Montreal, QC, Canada, 2020.

[8] Peng, Z., L. Li, M. Wang, Z. Zhang, Q. Liu, Y. Liu, and R. Liu, "An effective coverage scheme with passive-reflectors for urban millimeter-wave communication," *IEEE Antennas and Wireless Propagation Letters*, Vol. 15, 398–401, 2015.

[9] Shen, J., D. Zhu, B. Li, and P. Liang, "Repeater-enhanced millimeter-wave systems in multi-path environments," in *2015 IEEE 26th Annual International Symposium on Personal, Indoor, and Mobile Radio Communications (PIMRC)*, 769–774, Hong Kong, China, 2015.

[10] Li, L., Q. Chen, Q. Yuan, K. Sawaya, T. Maruyama, T. Furuno, and S. Uebayashi, "Frequency selective reflectarray using crossed-dipole elements with square loops for wireless communication applications," *IEEE Transactions on Antennas and Propagation*, Vol. 59, No. 1, 89–99, 2011.

[11] Raspopoulos, M. and S. Stavrou, "Frequency selective buildings through frequency selective surfaces," *IEEE Transactions on Antennas and Propagation*, Vol. 59, No. 8, 2998–3005, 2011.

[12] Ha, D., D. Choi, H. Kim, J. Kum, J. Lee, and Y. Lee, "Passive repeater for removal of blind spot in NLOS path for 5G fixed wireless access (FWA) system," in *2017 IEEE International Symposium on Antennas and Propagation & USNC/URSI National Radio Science Meeting*, 2049–2050, San Diego, CA, USA, 2017.

[13] Kim, B., H. Kim, D. Choi, Y. Lee, W. Hong, and J. Park, "28 GHz propagation analysis for passive repeaters in NLOS channel environment," in *2015 9th European Conference on Antennas and Propagation (EuCAP)*, 1–4, Lisbon, Portugal, Apr. 2015.

[14] Zhou, M., O. Borries, and E. Jørgensen, "Design and optimization of a single-layer planar transmit-receive contoured beam reflectarray with enhanced performance," *IEEE Transactions on Antennas and Propagation*, Vol. 63, No. 4, 1247–1254, 2015.

[15] Li, L., Q. Chen, Q. Yuan, K. Sawaya, T. Maruyama, T. Furuno, and S. Uebayashi, "Novel broadband planar reflectarray with parasitic dipoles for wireless communication applications," *IEEE Antennas and Wireless Propagation Letters*, Vol. 8, 881–885, 2009.

[16] Yu, N. and F. Capasso, "Flat optics with designer metasurfaces," *Nature Materials*, Vol. 13, No. 2, 139–150, 2014.

[17] Tang, W., J. Chen, and T. J. Cui, "Metamaterial lenses and their applications at microwave frequencies," *Advanced Photonics Research*, Vol. 2, No. 10, 2100001, 2021.

[18] Liu, L., X. Zhang, M. Kenney, X. Su, N. Xu, C. Ouyang, Y. Shi, J. Han, W. Zhang, and S. Zhang, "Broadband metasurfaces with simultaneous control of phase and amplitude," *Advanced Materials*, Vol. 26, No. 29, 5031–5036, 2014.

[19] Yi, H., J. Han, X. Ma, L. Li, and T. J. Cui, "Shaping flattened scattering patterns in broadband using passive reconfigurable intelligent surfaces for indoor NLOS wireless signal coverage enhancement," *ITU Journal on Future and Evolving Technologies*, Vol. 4, No. 1, 50–59, 2023.

[20] Guo, T., Y. Wang, L. Xu, M. Mei, J. Shi, L. Dong, Y. Xu, and C. Huang, "Joint communication and sensing design for multihop RIS-aided communication systems in underground coal mines," *IEEE Internet of Things Journal*, Vol. 10, No. 22, 19 533–19 544, 2023.

[21] Xue, H., Z. Lu, X. Ma, Z. Wang, L. Zhu, S. Yue, J. Han, H. Liu, and L. Li, "A reconfigurable metasurface enhancing signal coverage for wireless communication using reduced numbers of p-i-n diodes," *IEEE Transactions on Microwave Theory and Techniques*, Vol. 72, No. 3, 1964–1978, 2024.

[22] Wu, G.-B., S.-W. Qu, S. Yang, and C. H. Chan, "Broadband, single-layer dual circularly polarized reflectarrays with linearly polarized feed," *IEEE Transactions on Antennas and Propagation*, Vol. 64, No. 10, 4235–4241, 2016.